minerals

MDPI

*Article*

# Occurrence State and Enrichment Mechanism of Rhenium in the Qianjiadian Uranium Deposit in the Southwestern Songliao Basin, Northeast China

**Songlin Yang [1], Xingzhou Liu [1], Zhibo Shan [1], Angui Lei [1], Yong Liu [1], Da Wei [1], Shijiao Zhu [1], Yong Fu [1] and Long Zhang [2,*]**

[1] Exploration and Development Research Institute, Liaohe Oilfield Branch Company, PetroChina, Panjin 124010, China; yangsl1@petrochina.com.cn (S.Y.); liuxz@petrochina.com.cn (X.L.); sanzb@petrochina.com.cn (Z.S.); leiag@petrochina.com.cn (A.L.); liuyong6@petrochina.com.cn (Y.L.); weid1@petrochina.com.cn (D.W.); zhusj1@petrochina.com.cn (S.Z.); ful1@petrochina.com.cn (Y.F.)

[2] Shaanxi Key Laboratory of Petroleum Accumulation Geology, School of Earth Sciences and Engineering, Xi'an Shiyou University, Xi'an 710065, China

* Correspondence: longzhang@xsyu.edu.cn

**Abstract:** Rhenium is an extremely rare critical metal element in Earth's continental crust. Owing to its extremely high melting point and heat-stable crystalline structure, rhenium is an essential component of alloy materials used in high-performance aircraft engines. Demand for rhenium resources is therefore growing. Currently, most rhenium is produced as a byproduct of molybdenum mining in porphyry copper–molybdenum deposits. Research has therefore focused on the enrichment characteristics of rhenium in this type of deposit, with little attention paid to rhenium in other types of deposits. This study reports the occurrence state and enrichment mechanism of rhenium in the Qianjiadian sandstone-type uranium deposit in the Songliao Basin, Northeast China. Sequential extraction revealed that the average proportions of different forms of rhenium are as follows: water-soluble (57.86%) > organic-sulfide-bound (13.11%) > residual (12.26%) > Fe/Mn oxide-bound (10.67%) > carbonate-bound (6.10%). Combining mineralogical analysis techniques such as SEM-EDS, EMPA, and XRD, it has been established that rhenium does not occur as a substitute in sulfides (e.g., molybdenite) or uranium minerals in various types of deposits. Instead, it is mainly adsorbed onto clay minerals and Fe-Ti oxides, and in a small number of other minerals (pyrite, organic matter, and pitchblende). Rhenium is similar to redox-sensitive elements such as uranium and vanadium, and it is transported in a water-soluble form by oxidizing groundwater to the redox transition zone for enrichment. However, unlike uranium, which generally forms as uranium minerals, rhenium is mainly adsorbed and enriched onto clay minerals (kaolinite and interlayered illite–smectite). Most of the rhenium in sandstone-type uranium deposits occurs in an ion-adsorption state, and is easily leached and extracted during in-situ leaching mining of uranium ores. This type of deposit demonstrates excellent production potential and will become a crucial recoverable resource for future rhenium supply.

**Keywords:** rhenium; sequential extraction; sandstone-type uranium deposit; Qianjiandian deposit; Songliao Basin



**Citation:** Yang, S.; Liu, X.; Shan, Z.; Lei, A.; Liu, Y.; Wei, D.; Zhu, S.; Fu, Y.; Zhang, L. Occurrence State and Enrichment Mechanism of Rhenium in the Qianjiadian Uranium Deposit in the Southwestern Songliao Basin, Northeast China. *Minerals* **2024**, *14*, 67. https://doi.org/10.3390/min14010067

Academic Editor: Panagiotis Voudouris

Received: 6 November 2023
Revised: 28 December 2023
Accepted: 2 January 2024
Published: 5 January 2024



## 1. Introduction

Rhenium (Re) is one of the rarest elements in the Earth's crust, occurring in the upper crust at less than 1 ppb (part per billion) on average [1,2]. It has an extremely high melting point (~3180 °C) and a thermally stable crystalline structure, and is widely used in alloys for the turbine blades of high-performance aircraft engines and in catalysts for gasoline production [3]. At present, more than 80% of rhenium resources are used in the

manufacture of superalloys in the aerospace industry, 15% are used as catalysts in the petrochemical industry, and a small proportion are used in the manufacture of alloy materials for equipment in other fields, including electrical contacts, electromagnets, heating elements, mass spectrographs, semiconductors, thermocouples, and vacuum tubes [4]. Rhenium is regarded as a critical metal by many countries and institutions due to its important applications in the aerospace and petrochemical industries. With the rapid development of the aerospace industry, the global demand for rhenium resources will continue to increase.

Rhenium is an extremely rare, highly siderophile (ion attached), and chalcophile (S-attached, hence present in sulfide mineralization) element [5]. Due to the extremely rare nature of rhenium, Re-dominated minerals rarely form through geological processes. Although Re-dominated minerals do exist, such as rhenite ($ReS_2$, 74% Re), rhenium-rich tarkianite ((Cu, Fe)(Re, Mo)$_4S_8$, 49%–56% Re), and dzhezkazganite ($ReMoCu_2PbS_6$, 22% Re), they seldom form economically viable rhenium deposits [5,6]. Instead, most rhenium in nature substitutes for molybdenum in molybdenite. Thus, due to the similarity in charges and radii between rhenium and molybdenum, as well as their chalcophile nature, rhenium is usually enriched in molybdenite as a substitute ($ReS_2$) for molybdenum ($MoS_2$). The content of rhenium in various types of molybdenite varies greatly, ranging from less than 10 ppm to up to 11.5 wt%. Other minerals, such as uraninite and gadolinite, also contain rhenium due to substitution [3].

Currently, rhenium is primarily produced as a by-product of the production of molybdenum. Porphyry copper–molybdenum–gold deposits are the principal sources of rhenium, accounting for 80% of the total mining resources. In addition, rhenium enrichment is also observed in sedimentary copper mines and sandstone-type uranium deposits, such as the sandstone (red bed)-type copper mine in Kazakhstan, the reduced-facies (Kupferschiefer)-type copper–silver deposit in Poland, and the roll sandstone-type uranium deposit in Kazakhstan [3,7,8]. However, compared with rhenium in porphyry copper deposits, little attention has been paid to rhenium in sediment-hosted deposits, especially rhenium as a by-product of in-situ leaching of uranium in sandstone-type uranium deposits. The occurrence state and rhenium enrichment in uranium deposits are rarely reported, significantly impeding the exploration, assessment, and production of rhenium resources in this type of deposit.

The purpose of this paper is to characterize the specific features of rhenium enrichment compared to U ores in the Qianjiadian sandstone-type uranium deposit from southwestern Songliao Basin, China, and to investigate the enrichment mechanism of rhenium in sandstone-type uranium deposits. Sequential extraction and mineralogical analysis of rhenium provides vital information and a basis for the establishment of an enrichment model and in-situ leaching of rhenium in sandstone-type uranium deposits.

## 2. Geological Setting

### *2.1. Songliao Basin*

The Songliao Basin is a Cretaceous rift basin in Northeast China and is one of the largest continental sedimentary basins in the world, covering an area of 260,000 km$^2$ [9]. The basin is surrounded by the Great Xing'an Range to the west, the Lesser Xing'an Range to the northeast, the Zhangguangcai Range to the southeast, and the Kangping-Faku Hilly Area to the south. Based on the distribution pattern of uplifts and depressions, the basin is divided into seven first-order tectonic units: the western slope, the northern plunge, the central depression, the northeast uplift, the southeast uplift, the southwest uplift, and the Kailu Depression (Figure 1). The basement of the Songliao Basin is composed of Precambrian to Paleozoic metamorphic rocks, Paleozoic-Mesozoic granite, Paleozoic sedimentary strata, and Late Jurassic intermediate-acid volcanic rocks. Parts of the abovementioned rocks may have represented the primary uranium sources for uranium mineralization in the basin [10].

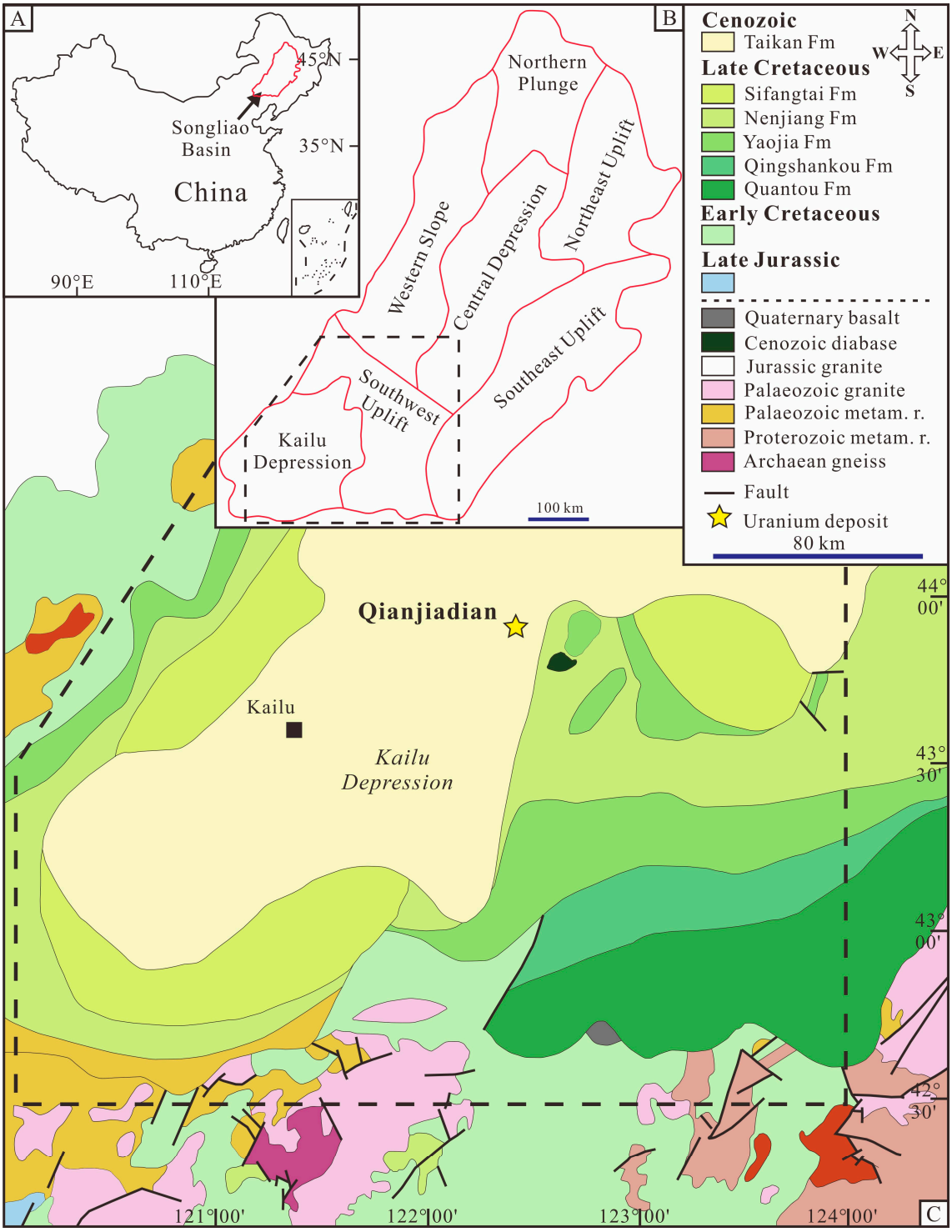


**Figure 1.** Location (**A**) and tectonic units (**B**) of the Songliao Basin. (**C**) Geological map of the Kailu Depression showing the location of the Qianjiadian uranium deposit (modified from [10]).

The Songliao Basin has experienced four geodynamic events: a prerift stage of mantle uplift and extensional faulting during the Late Jurassic; an Early Cretaceous syn-rift; a Late Cretaceous post-rift; and a Late Cretaceous-Cenozoic tectonic inversion [11–15]. The basin has a relatively complete and continuous Cretaceous continental sedimentary sequence up to 7000 m in thickness. The Shahezi ($K_1s$), Yingcheng ($K_1yc$), Denglouku ($K_1d$), and Quantou ($K_{1-2}q$) Formations developed from the bottom to the top during the Early Cretaceous syn-rift stage, and consist primarily of alluvial-fan, fluvial, deep lacustrine, and

pyroclastic sediments. The Qingshankou ($K_2q$), Yaojia ($K_2y$), Nenjiang ($K_2n$), Sifangtai ($K_2s$), and Mingshui ($K_2m$) Formations developed in the Late Cretaceous post-rift stage, and are mainly composed of alluvial-fan, fluvial, and shallow lacustrine-deep lacustrine sediments (Figure 2).

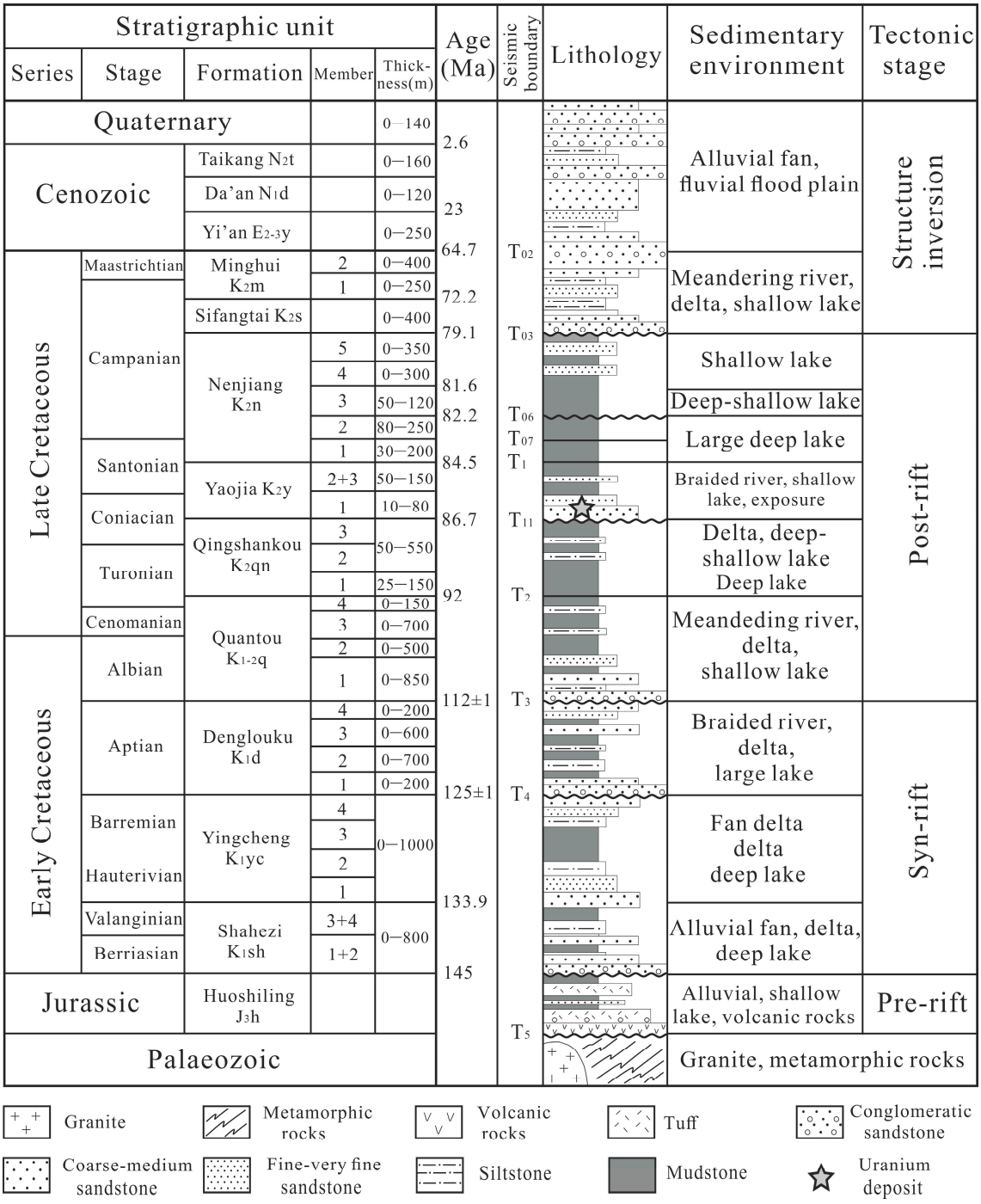


**Figure 2.** Stratigraphic column and tectonic evolution of the Songliao Basin (modified from [16]).

### *2.2. Qianjiadian Uranium Deposit*

The Qianjiadian uranium deposit lies in the Kailu Depression in the southwestern part of the basin, approximately 80 km to the northeast of Kailu city. The deposit is hosted in the Upper Cretaceous Yaojia Formation sandstone and is positioned over a depth interval between 200 and 500 m below the surface. The sedimentary period of the Yaojia Formation was the peak of the post-rift stage of the basin. The Qianjiadian area

developed braided delta sediments, mainly consisting of gray, gray-white, yellow, and red medium to fine-grained lithic feldspar sandstone and feldspathic litharenite interbedded with mudstones or argillaceous siltstones. The uranium mineralization primarily occurs in medium- to fine-grained sandstones. The spatial distribution of sandstone diagenetic facies shows that during the formation of the Qianjiadian sandstone-type uranium deposit, interlayer oxidation progressed from the southwest to the northeast. Along the direction of the interlayer oxidation, red sandstones, yellow sandstones, non-mineralized gray-white sandstones, mineralized gray sandstones, and primary gray sandstones occur in succession, corresponding to a complete oxidation zone, a partial evolution zone, a weak oxidation zone, a redox transition zone, and a reduction zone, respectively [17,18].

The uranium ore bodies are mostly tabular and lenticular in shape, with an average thickness of 5.1 m (Figure 3). The ore–hosting sandstone generally is gray adjacent to the upper red oxidation zone (Figure 4). Diabase dykes also occur near the uranium deposit, and previous studies have shown that some mineralized sandstones experienced hydrothermal alteration by hydrothermal fluids related to magmatic activity, resulting in dolomitization accompanied by U migration and deposition [19–22]. The average grade of the uranium ore is 0.024%, and the main uranium minerals are pitchblende and coffinite, with some brannerite. The spatial distributions of rhenium-bearing sandstones and uranium ore bodies are similar, and are located in the gray sandstone of the redox transition zone, with an average rhenium content of 447 ppb. However, the average rhenium contents of the red sandstones in the oxidation zone and the gray sandstones in the reduction zone are only 3 ppb and 6 ppb, respectively [23].

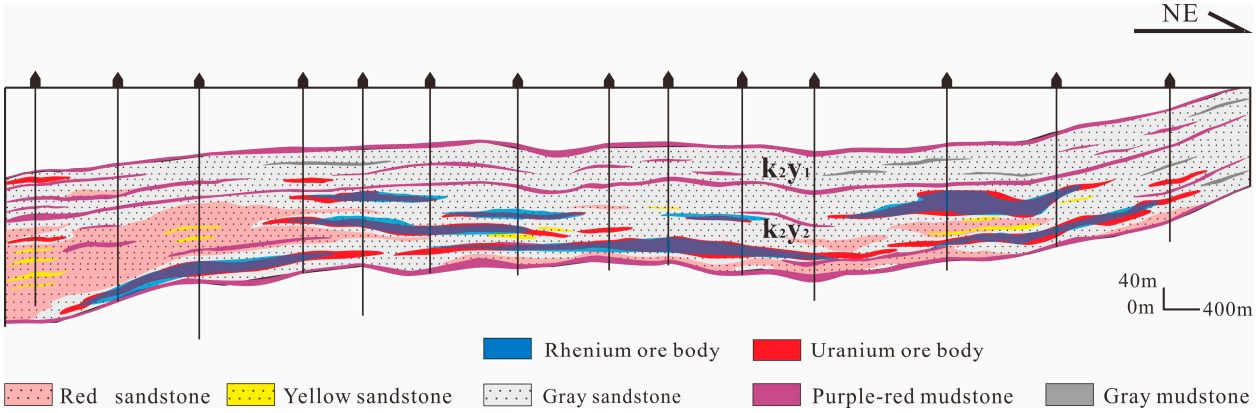


**Figure 3.** Cross-section showing the distribution of rhenium and uranium ores in the Qianjiadian uranium deposit.

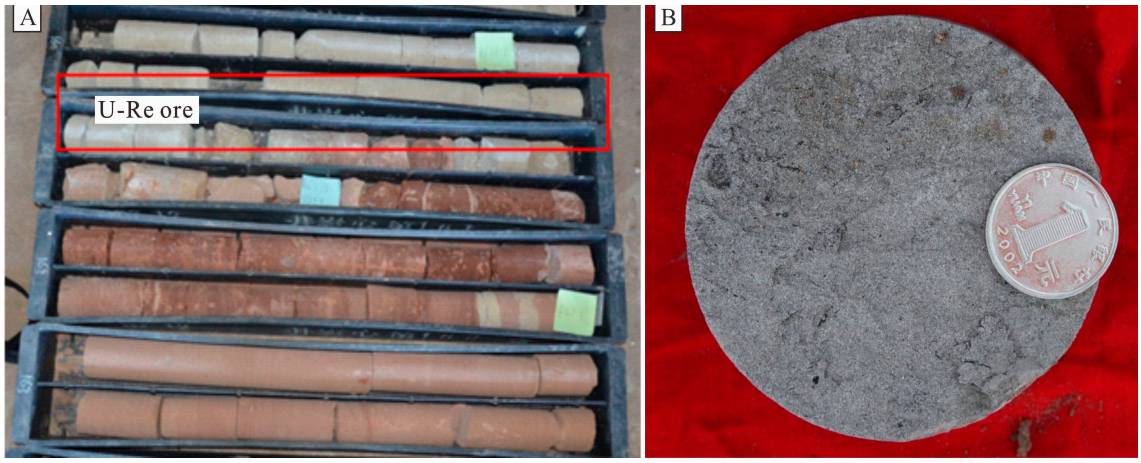


**Figure 4.** Drill cores from the Qianjiadian uranium deposit. (**A**) Uranium and rhenium ore located in the red to gray transition zone; (**B**) mineralized gray sandstone.

## 3. Materials and Methods

Eight gray sandstone samples from the redox transition zone of the Qianjiadian uranium deposit were selected for sequential chemical extraction of rhenium and uranium. The experiment was conducted at the Beijing Research Institute of Uranium Geology in Beijing, China, following Tessier's method [24]. Different forms of the metal elements Re and U were extracted, including soluble and exchangeable, carbonate-bound, Mn and Fe oxide-associated, organic-bound, and residual forms [24–29]. After each extraction step, centrifugal filtration and removal of liquid supernatants were carried out, and the rhenium and uranium contents in the solution were analyzed using high-resolution inductively coupled plasma mass spectrometry (HR-ICP-MS). The procedure was as follows: (1) to extract exchangeable Re and U, 20 mL of deionized water was added to the samples, which were then vigorously shaken at 20 °C for 24 h; (2) to extract the carbonate-bound parts, 20 mL 1 mol/L acetic acid solution was added, and the mixture was shaken well at 20 °C for 24 h; (3) to extract Fe/Mn oxide-bound Re and U, 20 mL 0.04 mol/L hydroxylamine hydrochloride solution was added, and the mixture was shaken well, and then oscillated for 24 h; (4) to extract the organic-pyrite-bound elements, 5 mL of 30% $H_2O_2$ solution and 5 mL of 0.2 mol/L $HNO_3$ solution were added, and the mixture was shaken well, and then placed in a constant temperature bath at 90 °C and intermittently stirred, followed by the addition of 10 mL of 3.2 mol/L $NH_4Ac$ solution, with the resulting mixture being shaken well; (5) the residual state was finally obtained by adding concentrated HF-$HC1O_4$ mixed solvent.

Polished thin sections of representative ore samples were selected for scanning electron microscopy (SEM) using an FEI Quanta 450 FEG instrument equipped with an energy dispersive spectrometer (EDS). The detection limits for Re and U are about 0.1 wt%. The mineral compositions were determined using a JEOL JXA–8230 electron microprobe (EMP) with an acceleration voltage of 15 kV, an analysis current of 20 nA, and a beam diameter of 1–5 μm. The analysis times were 10 s for the major elements, 20 s for minor elements, and 40 s for trace elements. The detection limit of EMPA for Re is about 0.02 wt%. SEM-EDS and EMP analyses were carried out at the State Key Laboratory of Continental Dynamics, Northwest University, Xi'an, China.

Clay minerals in the ore samples were determined via X-ray diffraction (XRD) analysis. Carbonate and organic matter was removed via acid treatment using acetic acid (15%) and hydrogen peroxide. Then, clay fractions were extracted through centrifugation. Samples of clay fraction (<2 μm fraction) were analyzed using a Rigaku D/max-2500 X-ray diffractometer at the Xi'an Center of Geological Survey, China. Clay minerals were identified from X-ray diffraction patterns of air-dried, ethylene glycol-solvated and heated samples for 2.5 h at 550 °C.

## 4. Results

### *4.1. Results of Chemical Sequential Extraction*

#### 4.1.1. Sequential Extraction of Rhenium

Exchangeable state (water-soluble fraction): In this study, by adding neutral deionized water, the metal elements were quickly extracted through external complexing action and diffusion. The results show that the proportions of rhenium in an exchangeable ion state range from 19.1% to 76.5%, averaging 57.9% (Table 1). In six of the eight samples, the proportion of rhenium in an exchangeable ion state exceeded 50.0%, indicating a predominant occurrence of rhenium at an adsorbed state on sediment surfaces within the Qianjiadian uranium deposit.

Carbonate-bound (weak acid-extractable fraction): Metal elements that co-precipitate with carbonate minerals—such as calcite or dolomite—were extracted using weakly acidic acetic acid. In every sample, the proportions of rhenium in the carbonate-bound state were the lowest of all types of forms, ranging from 2.8% to 9.4%, with an average of only 6.1%. This indicates that the co-precipitation of rhenium with carbonate minerals or its deposition of rhenium onto carbonate surface are rare.

**Table 1.** Re concentrations (ppb, $10^{-9}$) and proportion (%) obtained via sequential extractions of ore samples in the Qianjiadian uranium deposit.

| Sample No. | Total Re | Exchangeable Re | Carbonate-Bound Re | Re in Fe/Mn Oxide | Organic-Pyrite-Bound Re | Residual Re |
|---|---|---|---|---|---|---|
| Q2021-18 | 956 | 720 (75.4%) | 41 (4.3%) | 46 (4.8%) | 61 (6.4%) | 88 (9.2%) |
| Q2021-21 | 1011 | 750 (74.2%) | 93 (9.2%) | 61 (6.0%) | 40 (4.0%) | 67 (6.6%) |
| Q2021-35 | 95 | 34 (35.6%) | 9 (9.4%) | 12 (12.9%) | 11 (11.4%) | 29 (30.7%) |
| Q2021-56 | 938 | 648 (69.1%) | 52 (5.5%) | 67 (7.1%) | 102 (10.9%) | 70 (7.4%) |
| Q2021-93 | 173 | 99 (57.1%) | 8 (4.4%) | 10 (5.6%) | 47 (27.0%) | 10 (6.0%) |
| Q2021-111 | 355 | 199 (56.0%) | 16 (4.6%) | 25 (7.1%) | 46 (13.0%) | 68 (19.3%) |
| Q2021-115 | 664 | 127 (19.1%) | 57 (8.6%) | 242 (36.5%) | 134 (20.2%) | 104 (15.7%) |
| Q2021-167 | 258 | 197 (76.5%) | 7 (2.8%) | 14 (5.4%) | 31 (12.0%) | 8 (3.3%) |
| Mean | | 57.9% | 6.1% | 10.7% | 13.11% | 12.3% |

Fe/Mn oxide-bound (reducible fraction): The most effective reagents for extracting metal ions in the Fe/Mn oxide-bound state are reducing agents and ligands that release ions in solution [29]. The most common reduction process for dissolving Fe/Mn oxides is hydroxylamine extraction, using hydroxylamine hydrochloride [30]. With the exception of one sample (Sample no. Q2021-115) displaying a high rhenium content, the proportion of rhenium in the Fe/Mn oxide-bound state within the Qianjiadian uranium deposit was relatively low, averaging 10.7%. In most samples, the proportion of rhenium in the Fe/Mn oxide-bound state was less than 10.0%.

Organic-pyrite-bound (Re fraction liberated after oxidation): Metal elements encapsulated by organic matter and pyrite can be dissolved and precipitated by oxidants, with hydrogen peroxide being the most commonly used. $H_2O_2$ also has a certain degree of reducibility, so it can reduce $MnO_2$ in an environment at a pH lower than 5. This step is therefore normally carried out after the extraction of Fe/Mn oxide-bound metals. The results show that the proportion of rhenium in the organic-pyrite-bound state in mineralized sandstones in the study area ranges from 4.0% to 27.0%, with an average of 13.1%.

Residual state: Metal elements contained in a mineral lattice generally occur in silicate minerals and metal minerals, which can be extracted using strong acids. Rhenium does not easily form minerals of its own, and residual rhenium mainly occurs in silicate and uranium minerals as a result of substitution. The proportion of residual-state rhenium ranges from 3.3% to 30.7%, with an average of 12.3%. Apart from sample Q2021-35, where the proportion of residual-state rhenium reached 30.7%, the content in the remaining samples was relatively low.

The average proportions of rhenium obtained via sequential extraction from the Qianjiadian sandstone-type uranium deposit are as follows: water-soluble state (57.9%) > organic-sulfide-bound state (13.1%) > residual state (12.3%) > Fe/Mn oxide-bound state (10.7%) > carbonate-bound state (6.1%). The water-soluble rhenium predominates in the sandstone-type uranium deposit, while other forms of rhenium are relatively low in proportion (Figure 5). This contrasts with porphyry copper–molybdenum deposits, where rhenium mainly occurs as a substitute for molybdenum within molybdenite.

#### 4.1.2. Sequential Extraction of Uranium

To determine the enrichment and mineralization relationship between rhenium and uranium in sandstone-type uranium deposits, a sequential extraction of uranium was conducted on the same ore samples. The average proportions of uranium of the five distinctive states were as follows: Fe/Mn oxide-bound state (47.8%) > carbonate-bound state (20.8%) > organic-pyrite-bound state (11.7%) > water-soluble state (11.1%) > residual state (8.6%) (Table 2). The sequential extraction results for uranium differ fundamentally from those of rhenium, with uranium predominantly present in the Fe/Mn oxide-bound and carbonate-bound states, while the proportion of uranium enriched in the water-soluble state is relatively low (Figures 6 and 7).

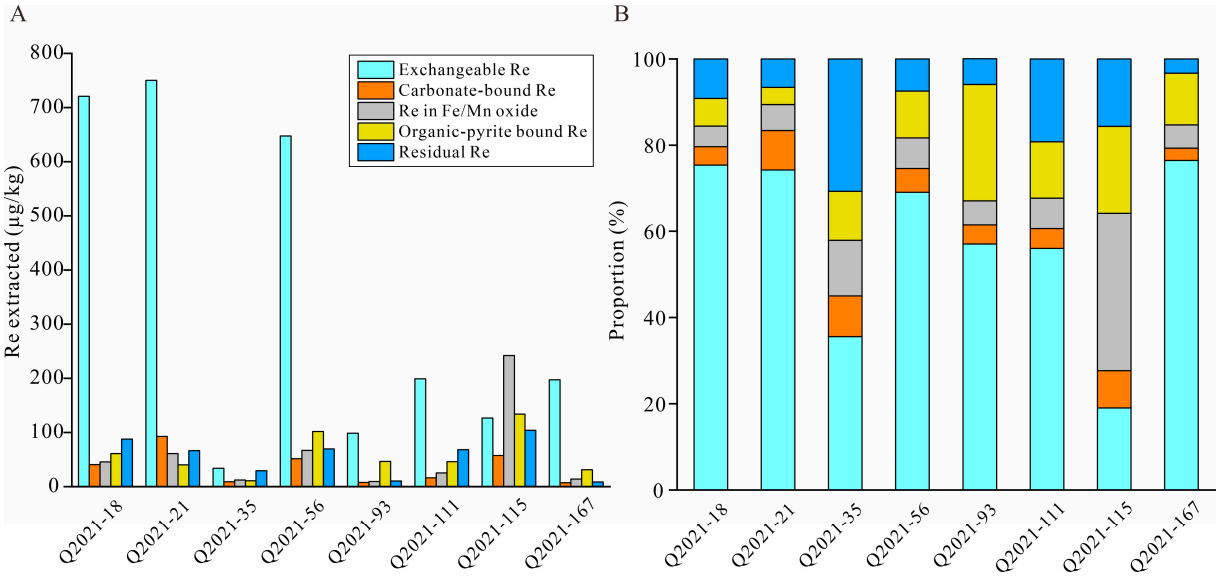


**Figure 5.** Concentrations (**A**) and proportion (**B**) of rhenium in gray sandstones from the redox transition zone in the Qianjiadian uranium deposit determined by sequential extraction procedures.

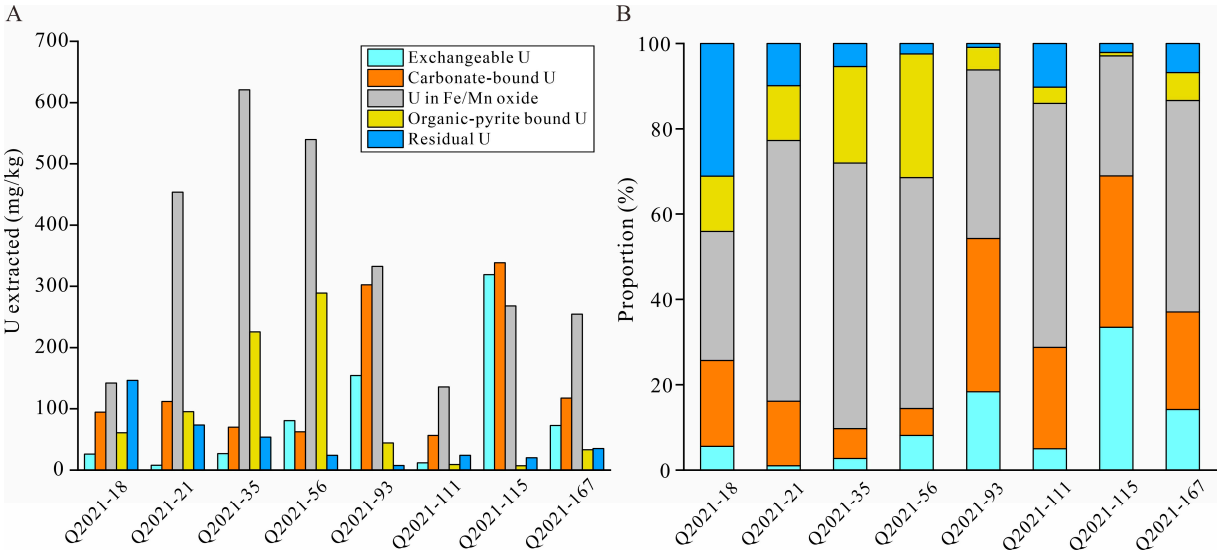


**Figure 6.** Concentrations (**A**) and proportion (**B**) of uranium in gray sandstones from the redox transition zone in the Qianjiadian uranium deposit established by sequential extraction.

**Table 2.** U concentrations (ppm, $10^{-6}$) and proportion (%) obtained by sequential extractions of uranium ore samples in the Qianjiadian uranium deposit.

| Sample No. | Total U | Exchangeable U | Carbonate-Bound U | U in Fe/Mn Oxide | Organic-Pyrite-Bound U | Residual U |
|---|---|---|---|---|---|---|
| Q2021-18 | 470.5 | 26.2 (5.6%) | 94.8 (20.1%) | 142.1 (30.2%) | 61.1 (13.0%) | 146.3 (31.1%) |
| Q2021-21 | 742.7 | 7.8 (1.0%) | 112.2 (15.1%) | 453.6 (61.1%) | 95.4 (12.8%) | 73.7 (9.9%) |
| Q2021-35 | 997.5 | 27.0 (2.7%) | 70.1 (7.0%) | 621.0 (62.3%) | 225.6 (22.6%) | 53.9 (5.4%) |
| Q2021-56 | 996.7 | 80.9 (8.1%) | 62.8 (6.3%) | 539.8 (54.2%) | 289.0 (29.0%) | 24.2 (2.4%) |
| Q2021-93 | 841.3 | 154.5 (18.4%) | 302.4 (35.9%) | 332.4 (39.5%) | 44.3 (5.3%) | 7.7 (0.9%) |
| Q2021-111 | 237.7 | 11.9 (5.0%) | 56.5 (23.8%) | 135.9 (57.2%) | 9.1 (3.8%) | 24.3 (10.2%) |
| Q2021-115 | 953.3 | 319.0 (33.5%) | 338.5 (35.5%) | 268.2 (28.1%) | 7.2 (0.8%) | 20.4 (2.1%) |
| Q2021-167 | 513.9 | 73.0 (14.2%) | 117.5 (22.9%) | 254.7 (49.6%) | 33.4 (6.5%) | 35.2 (6.9%) |
| Mean | | 11.1% | 20.8% | 47.8% | 11.7% | 8.6% |

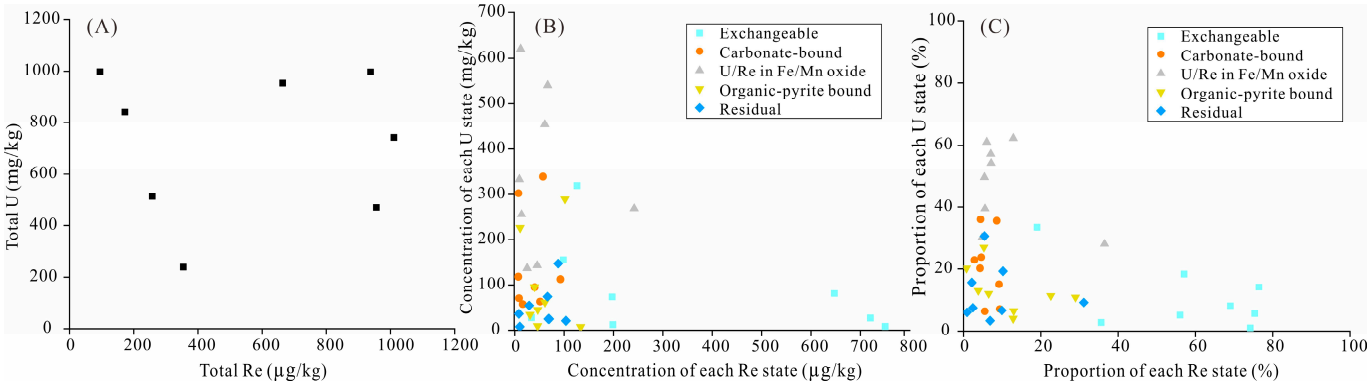


**Figure 7.** Diagrams showing the extracted Re and U of different phases in the Re-U ore samples. (**A**) Total Re vs. total U; (**B**) concentrations of each Re state vs. each U state; (**C**) proportion of each Re state vs. each U state.

### *4.2. Mineralogical Characteristics*

#### 4.2.1. Image Analysis

The rhenium contents of various minerals were determined using SEM-EDS. Energy spectrum analyses of diverse minerals determined that the principal minerals containing rhenium are clay minerals (kaolinite and illite–smectite mixed layer mineral), Fe-Ti oxides (mainly ilmenite and magnetite), pyrite, and pitchblende. Clay minerals and Ti/Fe oxides are the main host minerals for rhenium, and rhenium is readily detectable in these minerals (Figure 8A,B). Fe-Ti oxides have widely experienced intense alteration, resulting in significant iron depletion, and some of them have undergone replacement by pyrite and pitchblende. Moreover, Ti-Fe oxides containing rhenium also contain a certain amount of vanadium. By contrast, the oxidation zone only contains very small amounts of Fe-Ti oxides, which have mostly undergone strong oxidation and alteration by oxidized groundwater and have been converted into hematite, which does not contain rhenium. Although pyrite is widely developed in mineralized sandstones in the redox transition zone, only a small proportion of pyrite contains rhenium (Figure 8C). In addition, accessory minerals such as zircon, monazite, and apatite also contain trace amounts of rhenium (Figure 8D). The content of all these accessory minerals in the sandstone is very low, and there is no evidence to suggest that they undergo alteration during oxidation or reduction. The trace rhenium in these accessory minerals may therefore be fixed in the mineral lattice and unavailable to release and participate in rhenium enrichment and in-situ leaching mining. In some mineralized sandstones, organic matter debris is present, and rhenium may exist in an adsorption state on the surface of organic matter. However, rhenium content within organic matter falls below the detection limits of energy-dispersive X-ray spectroscopy and electron probe microanalysis. Further accurate in situ analysis of trace elements is needed to determine the contents of rhenium in organic matter.

#### 4.2.2. EMPA of Uranium Minerals

The uranium-bearing minerals in mineralized sandstones are primarily pitchblende and coffinite, with small amounts of brannerite. Figure 9 shows the close association of uranium minerals with framboidal pyrite and Fe-Ti oxides. Electron microprobe analysis of the uranium minerals in mineralized zones was carried out. The results indicate that pitchblende commonly contains rhenium (Table 3), ranging from 0.47 wt% to 0.61 wt%, and trace amounts of rhenium are also present in brannerite. Rhenium were generally not detected in coffinite, where the content of FeO and ZrO is relatively high (up to 9.30 wt% and 11.88 wt%, respectively), whereas in pitchblende, the contents of FeO and ZrO are notably lower, ranging below 1.51 wt% and 1.44 wt%, respectively.

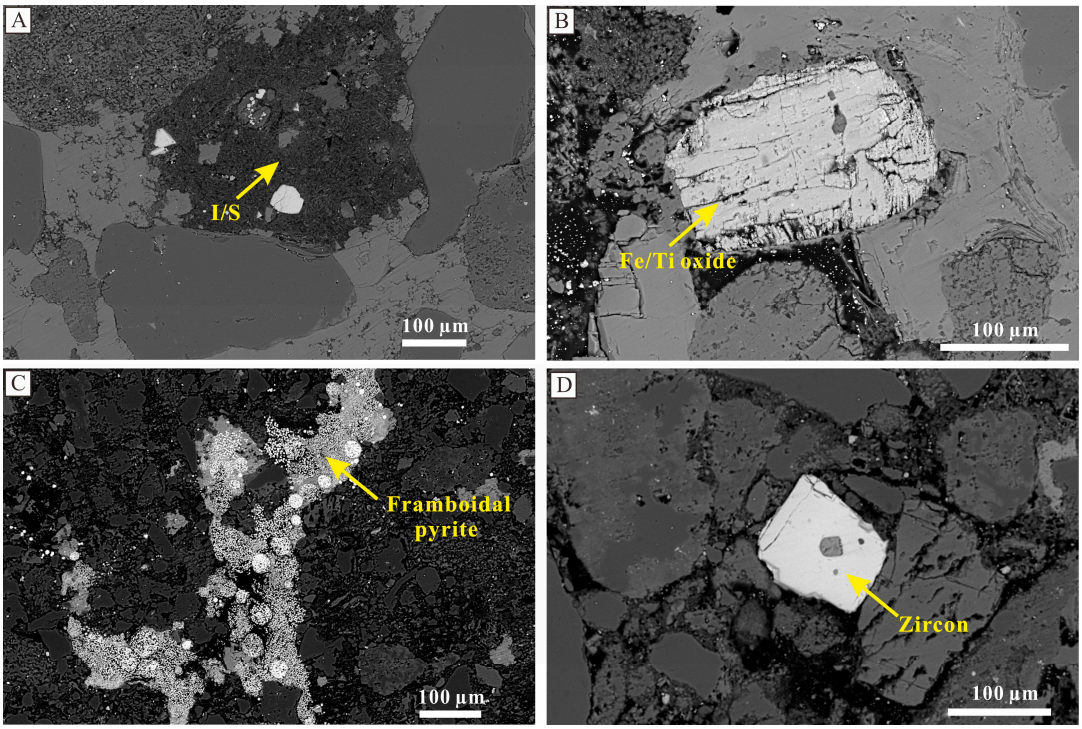


**Figure 8.** Host minerals for rhenium in the sandstone from the Qianjiadian uranium deposit. Back-scattered electron images showing the Re-bearing minerals. (**A**) Clay mineral (interlayered illite–smectite (I/S)); (**B**) Fe-Ti oxide; (**C**) pyrite; (**D**) zircon.

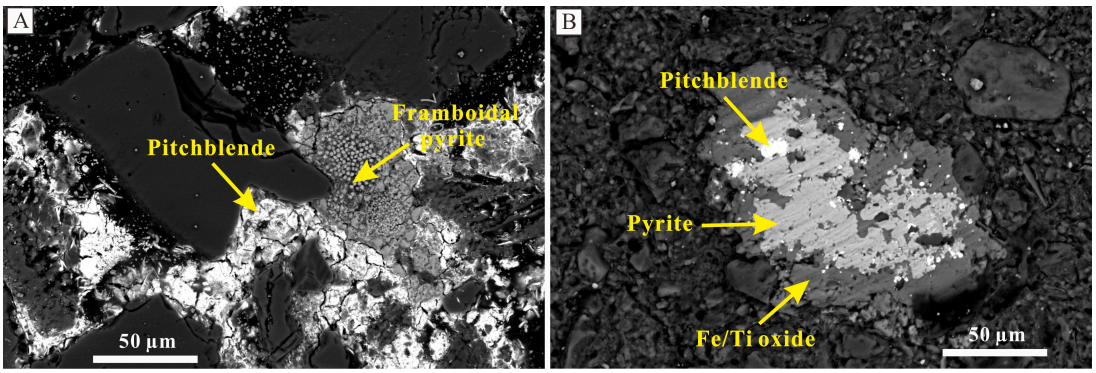


**Figure 9.** Back-scattered electron images displaying the uranium minerals from the Qianjiadian deposit. (**A**) Pitchblende associated with framboidal pyrite. (**B**) Pitchblende and pyrite replacement on altered Ti/Fe-oxide.

**Table 3.** EMPA results for uranium minerals in the Qianjiadian deposit (composition in wt%; bdl, below detection limit).

| Analysis No. | $SiO_2$ | $P_2O_5$ | $Al_2O_3$ | $Na_2O$ | $TiO_2$ | MnO | FeO | CaO | $K_2O$ | $UO_2$ | PbO | $ReO_2$ | $ZrO_2$ | Total | Type of Mineral |
|---|---|---|---|---|---|---|---|---|---|---|---|---|---|---|---|
| Q2021-143-1 | 0.67 | 2.08 | 0.07 | 0.25 | bdl | 0.34 | 1.15 | 4.41 | bdl | 68.41 | bdl | 0.61 | 0.95 | 78.95 | pitchblende |
| Q2021-143-2 | 1.14 | 2.76 | 0.14 | 0.70 | bdl | 0.47 | 0.85 | 5.19 | bdl | 70.83 | 0.03 | 0.54 | 1.20 | 83.84 | pitchblende |
| Q2021-167-4 | 0.68 | 1.39 | 0.01 | 0.79 | 0.30 | 0.13 | 1.51 | 4.04 | bdl | 78.58 | 0.02 | 0.47 | 1.44 | 89.35 | pitchblende |
| Q2021-51-1 | 15.71 | 4.20 | 6.26 | 0.08 | 0.05 | 0.01 | 2.89 | 3.32 | 0.38 | 48.62 | 0.01 | bdl | 1.79 | 83.31 | coffinite |
| Q2021-170-3 | 16.21 | 6.37 | 2.90 | 0.53 | bdl | 0.11 | 9.30 | 2.60 | bdl | 37.89 | 0.12 | bdl | 11.14 | 87.17 | coffinite |
| Q2021-170-4 | 14.51 | 5.58 | 3.39 | 0.41 | 0.15 | 0.01 | 8.63 | 2.77 | bdl | 37.65 | bdl | bdl | 11.88 | 84.98 | coffinite |
| Q2021-167-1 | 0.89 | 0.67 | 0.34 | 0.76 | 50.15 | 0.11 | 3.67 | 1.21 | bdl | 18.09 | 0.05 | 0.12 | 1.51 | 77.58 | brannerite |
| Q2021-167-2 | 1.13 | 1.12 | 0.32 | 1.20 | 47.31 | 0.13 | 3.87 | 1.52 | bdl | 24.16 | bdl | 0.05 | 2.14 | 82.94 | brannerite |

4.2.3. Characteristics of Clay Minerals

XRD further revealed the contents of clay minerals in the ore samples (Table 4). Kaolinite was the dominant clay mineral in all samples, ranging from 55% to 72% (average = 61%). Kaolinite occurred as vermiform crystals filling in the intergranular pores. The second-most abundant clay mineral is the interlayered illite–smectite, ranging from 20% to 30% (average = 26%). The relative contents of illite and chlorite in the ore samples are relatively lower. Smectite is rarely observed in all samples.

**Table 4.** Clay mineral contents (%) of the U-Re ore samples tested by X-ray diffraction analysis in the Qianjiadian uranium deposit.

| Analysis No. | Smectite | Interlayered Illite–Smectite | Illite | Kaolinite | Chlorite |
|---|---|---|---|---|---|
| Q2021-18 | 0 | 28 | 13 | 55 | 4 |
| Q2021-21 | 0 | 23 | 4 | 65 | 8 |
| Q2021-35 | 0 | 27 | 5 | 57 | 11 |
| Q2021-56 | 0 | 27 | 0 | 65 | 8 |
| Q2021-93 | 0 | 27 | 6 | 58 | 9 |
| Q2021-111 | 0 | 30 | 6 | 55 | 9 |
| Q2021-115 | 0 | 20 | 3 | 72 | 5 |
| Q2021-167 | 0 | 22 | 6 | 62 | 10 |
| Mean | 0 | 26 | 6 | 61 | 8 |

## 5. Discussion

### *5.1. Occurrence of Rhenium in the Qianjiadian Uranium Deposit*

The nature of the occurrence of rhenium in sandstone-type uranium deposits is not well understood, with limited specialized research on this topic. Some researchers have speculated that rhenium may be enriched in jordisite, an amorphous molybdenum mineral with a composition similar to molybdenite, based on the co-occurrence of rhenium and molybdenum in uranium deposits [31]. Additionally, due to the close association between the distributions of rhenium and uranium, it has been suggested that rhenium may be enriched in uranium minerals such as uraninite [31,32]. The results of this study, combining chemical sequential extraction, SEM-EDS, EMPA, and XRD, indicate that molybdenite, a rhenium-enriched mineral, is absent in sandstone-type uranium deposits. Sequential extraction experiments reveal that water-soluble rhenium accounts for an average of over 57.9%. Rhenium bound to Fe/Mn oxide and organic sulfide may also contain some rhenium in the ion-adsorption state, suggesting that most rhenium is present as ion-adsorbed species. Conversely, a substantial portion of uranium is found in the solid phase, with its adsorption state being comparatively less prevalent (Figure 7). It is speculated that the rhenium-bearing minerals include clay minerals (kaolinite and interlayered illite–smectite), Ti-Fe oxides, and minor quantities of organic matter, pyrite, and uranium minerals, with the ion-adsorbed rhenium mainly present on the surfaces of clay minerals.

Clay minerals exhibit significant enrichment capacity for rhenium. The most recent study on the enrichment of rhenium in the Wuliping Pb-Zn-Mo polymetallic deposit in Guizhou Province, South China revealed that in the rhenium-enriched mudstone samples within the deposit, rhenium was mainly adsorbed onto kaolinite [33]. These rhenium-enriched samples have undergone strong weathering processes. The enrichment process of rhenium involves the release and migration of rhenium from molybdenite in the primary hydrothermal deposit to eventually be adsorbed and enriched by clay minerals under supergene oxidation conditions. Kaolinite and interlayered illite–smectite possess large specific-surface and ion-exchange capacity, making them the main host minerals for rhenium. Our results also support the understanding that, in epigenetic sandstone-type uranium deposits, rhenium predominantly exists in the form of ion adsorption and is enriched on the surfaces of clay minerals (kaolinite and interlayered illite–smectite). The content of clay minerals in the Qianjiadian uranium deposit reaches 20%–30% of the total mineral content in the sandstone [20], allowing for substantial adsorption of rhenium.

Additionally, X-ray energy spectrum scanning analysis results indicate that Fe-Ti oxides in the Qianjiadian uranium deposit also contain a certain amount of rhenium. Previous studies have shown that uranium may be reduced as nanocrystals in Fe-Ti oxides [10,34,35], suggesting that these minerals effectively enrich redox-sensitive elements, such as rhenium and uranium, near redox boundaries. Currently, there is no evidence indicating that pyrite can effectively enrich rhenium. We only detected Re in a small portion of pyrite, indicating that pyrite is not the main host mineral. The low proportion of organic-pyrite-bound rhenium in sequential extraction experiments further confirms this finding.

Sequential extraction analysis of uranium reveals that there are significant differences between the occurrence states of uranium and rhenium (Figure 7B,C). Uranium primarily exists in uranium minerals, Fe-Ti oxides, and carbonate-bound uranium. Among uranium minerals, pitchblende contains rhenium, but only in small proportions. The absence of rhenium in coffinite may be related to the hydrothermal origin of coffinite in the Qianjiadian deposit [36]. Hydrothermal fluids produced by the intrusion of diabase exhibit weak reduction, making them ineffective in transporting redox-sensitive elements such as rhenium and vanadium. However, uranium is more sensitive to redox change than rhenium and vanadium, and small changes in the reduction–oxidation conditions of the fluid can cause U to be more soluble relative to Re and V [37]. Although the spatial distribution of uranium and rhenium in uranium deposits appears relatively consistent, the uranium and rhenium contents in mineralized rocks do not exhibit a significantly positive correlation (Figure 7A) [23]. This finding also indicates that uranium minerals are not the main host minerals for rhenium. The enriched rhenium in uranium mineralized sandstones with extremely high uranium content probably comes from the rhenium in pitchblende. Most of the rhenium in the redox zone is still in the form of an ion-adsorption state.

### *5.2. Enrichment of Rhenium and Implications for In-Situ Leaching*

Rhenium exhibits several valences from −1 to +7, with the most common being +7, +6, +4, and +2. Sandstone-type uranium deposits often exhibit enrichment of rhenium, mainly concentrated within the oxidation–reduction transition zones. In oxidizing environments, rhenium is activated into $Re^{7+}$ ions and dissolves in oxidizing groundwater. Under confined conditions, rhenium-bearing groundwater infiltrates, leading to a series of physical and chemical reactions with surrounding rocks, resulting in geochemical zonation. When the fluid migrates to a redox transition zone, the $Re^{7+}$ in the fluid is reduced to $Re^{4+}$ by reducing agents such as organic matter (for example, coal debris and hydrocarbons) and pyrite. This reduction leads to decreased ionic activity and mobility, causing rhenium to adsorb onto clay minerals, similar to the ore-forming process of uranium mineralization. In addition to Re, redox transition zones often exhibit the enrichment of elements such as uranium, selenium, vanadium, and molybdenum [37,38]. Enrichment of these elements has also been observed in other rhenium deposits associated with epigenetic fluids, such as the Wuliping ion-adsorption rhenium deposit in South China [33], and the roll-front type uranium deposit in the Chu-Sarysu Basin, Kazakhstan [8]. In this environment, the enrichment of rhenium differs from that of uranium, molybdenum, and other elements. Rhenium is less likely to form substantial Re minerals or substitute in the mineral lattice (e.g., pitchblende and molybdenite). Instead, it mainly exists in an ion-adsorption state on the surfaces of clay minerals and Fe-Ti oxides. Although the spatial distribution of these redox-sensitive elements is generally consistent, there is no obvious positive correlation between the relative contents of these elements in the samples because of variations in their occurrence states, redox sensitivity, and the degree of alteration by late-stage fluid processes. Consequently, the concentrations of these elements in samples do not exhibit a distinct positive correlation.

In the Qianjiadian sandstone-type uranium deposit, rhenium is rarely present in the form of substitution within sulfides and uranium minerals. Instead, it predominantly occurs in an ion-adsorption state. Sequential extraction shows that around 57% of rhenium can be dissolved in neutral water. The proportions of rhenium in the carbonate-bound

and organic-sulfide states obtained after weak acidification and oxidation are 13.1% and 6.1%, respectively. This suggests that more than 70% of rhenium can be extracted by in-situ leaching mining using acidification and oxidation for uranium production. In most of the world's sandstone-type uranium deposits, no attention has been given to the potential for in-situ leaching mining of rhenium as a by-product. At present, only approximately 1% of rhenium production comes from sandstone-type uranium deposits [3]. Rhenium in such deposits is mainly adsorbed by clay minerals and Ti-Fe oxides, demonstrating excellent exploitation and production potential. This portion of recoverable resources has been seriously neglected and underestimated.

## 6. Conclusions

Rhenium is concentrated within the gray sandstone in the redox transition zone of the Qianjiadian sandstone-type uranium deposit. Our research indicates that rhenium mainly occurs in an ion-adsorption state, which is different from the occurrence characteristics of rhenium in most rhenium-bearing deposits, where it substitutes for other elements in molybdenite or uranium minerals. The main host minerals of rhenium in sandstone-type uranium deposits are clay minerals (kaolinite and interlayered illite–smectite) and Ti-Fe oxides, along with small amounts of pyrite, organic matter, and pitchblende. Oxidizing groundwater carries soluble high-valence uranium, rhenium, and vanadium into the redox transition zone, where they are reduced to their low valence by reducing agents such as organic matter and pyrite, resulting in their enrichment. However, the occurrence states of these elements significantly differ. The proportion of water-soluble rhenium in the sandstone-type uranium deposits averages 57.9%, and the leaching fraction of rhenium after acidification and oxidation exceeds 70%. Most of the rhenium can be extracted during the in-situ leaching of uranium ore, which therefore has excellent Re recovery potential. Rhenium in sandstone-type uranium deposits has not previously been widely studied or considered as a valuable resource. Nevertheless, this type of deposit may emerge as a crucial alternative source to the main rhenium production from porphyry copper–molybdenum deposits in the future.

**Author Contributions:** Conceptualization, S.Y. and L.Z.; methodology, S.Y., X.L. and D.W.; software, L.Z.; formal analysis, S.Y.; investigation, S.Y., X.L., Z.S., A.L., Y.L., D.W., S.Z., Y.F. and L.Z.; resources, S.Y. and L.Z.; writing—original draft preparation, S.Y. and L.Z.; writing—review and editing, L.Z.; visualization, S.Y., X.L., Z.S., A.L., Y.L., D.W., Y.F. and L.Z.; supervision, S.Y. and L.Z.; project administration, S.Y.; funding acquisition, S.Y. and L.Z. All authors have read and agreed to the published version of the manuscript.

**Funding:** This research was funded by the Scientific Research and Technology Development Project of PetroChina, grant number 2021DJ5301, and the National Natural Science Foundation of China, grant number 42302176.

**Data Availability Statement:** The data presented in this study are available upon request from the corresponding author.

**Conflicts of Interest:** Authors have received research grants from Liaohe Oilfield Branch Company. The authors declare no conflicts of interest.

## References

1. Taylor, S.R.; Mclennan, S.M. The Geochemical the Continental Evolution Crust. *Rev. Mineral. Geochem.* **1995**, *33*, 241–265. [CrossRef]
2. Rudnick, R.L.; Gao, S. Composition of the Continental Crust. In *Treatise on Geochemistry*; Holland, H.D., Turekian, K.K., Eds.; Elsevier-Pergamon: Oxford, UK, 2003; Volume 3, pp. 1–64.
3. John, D.A.; Seal, R.R., II; Polyak, D.E. Rhenium. In *Critical Mineral Resources of the United States—Economic and Environmental Geology and Prospects for Future Supply*; Schulz, K.J., DeYoung, J.H., Seal, R.R., II, Bradley, D.C., Eds.; U.S. Geological Survey Professional Paper 1802: Reston, VA, USA, 2017; pp. 1–49. [CrossRef]
4. Werner, T.T.; Mudd, G.M.; Jowitt, S.M.; Huston, D. Rhenium mineral resources: A global assessment. *Resour. Policy* **2023**, *82*, 103441. [CrossRef]

5. Brenan, J.M. Rhenium. In *Encyclopedia of Geochemistry: A Comprehensive Reference Source on the Chemistry of the Earth*; White, W.M., Ed.; Springer International Publishing: Cham, Switzerland, 2018; pp. 1312–1314.
6. Kojonen, K.K.; Roberts, A.C.; Isomaki, O.-P.; Knauf, V.V.; Johanson, B.; Pakkanen, L. Tarkianite, (Cu,Fe) $(Re,Mo)_4S_8$, a new mineral species from the Hitura Mine, Nivala, Finland. *Can. Miner.* **2004**, *42*, 539–544. [CrossRef]
7. Hitzman, M.; Kirkham, R.; Broughton, D.; Thorson, J.; Selley, D. The sediment-hosted stratiform copper ore system. In *Economic Geology One Hundredth Anniversary Volume 1905–2005*; Hedenquist, J.W., Thompson, J.F.H., Goldfarb, R.J., Richards, J.P., Eds.; Society of Economic Geologists, Inc.: Littleton, CO, USA, 2005; pp. 609–642. [CrossRef]
8. Dahlkamp, F.J. (Ed.) *Uranium Deposits of the World*; Springer: Berlin/Heidelberg, Germany, 2009; pp. 1–493.
9. Song, Y.; Ren, J.; Stepashko, A.A.; Li, J. Post-rift geodynamics of the Songliao Basin, NE China: Origin and significance of T11 (Coniacian) unconformity. *Tectonophysics* **2014**, *634*, 1–18. [CrossRef]
10. Bonnetti, C.; Liu, X.; Zhaobin, Y.; Cuney, M.; Michels, R.; Malartre, F.; Mercadier, J.; Cai, J. Coupled uranium mineralisation and bacterial sulphate reduction for the genesis of the Baxingtu sandstone-hosted U deposit, SW Songliao Basin, NE China. *Ore Geol. Rev.* **2017**, *82*, 108–129. [CrossRef]
11. Song, Y.; Ren, J.; Liu, K.; Lyu, D.; Feng, X.; Liu, Y.; Stepashko, A. Syn-rift to post-rift tectonic transition and drainage reorganization in continental rifting basins: Detrital zircon analysis from the Songliao Basin, NE China. *Geosci. Front.* **2022**, *13*, 101377. [CrossRef]
12. Liu, C.; Shan, X.; Yi, J.; Shi, Y.; Ventura, G. Volcanism at the end of continental rifting: The Cretaceous syn-rift to post-rift transition in the Songliao Basin (NE China). *Gondwana Res.* **2022**, *111*, 174–188. [CrossRef]
13. Liu, C.; Nicotra, E.; Shan, X.; Yi, J.; Ventura, G. The Cretaceous volcanism of the Songliao Basin: Mantle sources, magma evolution processes and implications for the NE China geodynamics—A Review. *Earth-Sci. Rev.* **2023**, *237*, 104294. [CrossRef]
14. Li, Z.; Chen, J.; Zou, H.; Wang, C.; Meng, Q.; Liu, H.; Wang, S. Mesozoic–Cenozoic tectonic evolution and dynamics of the Songliao Basin, NE Asia: Implications for the closure of the Paleo-Asian Ocean and Mongol-Okhotsk Ocean and subduction of the Paleo-Pacific Ocean. *Earth-Sci. Rev.* **2021**, *218*, 103471. [CrossRef]
15. Wang, P.-J.; Mattern, F.; Didenko, N.A.; Zhu, D.-F.; Singer, B.; Sun, X.-M. Tectonics and cycle system of the Cretaceous Songliao Basin: An inverted active continental Margin Basin. *Earth-Sci. Rev.* **2016**, *159*, 82–102. [CrossRef]
16. Zhao, L.; Cai, C.; Jin, R.; Li, J.; Li, H.; Wei, J.; Guo, H.; Zhang, B. Mineralogical and geochemical evidence for biogenic and petroleum-related uranium mineralization in the Qianjiadian deposit, NE China. *Ore Geol. Rev.* **2018**, *101*, 273–292. [CrossRef]
17. Rong, H.; Jiao, Y.; Wu, L.; Wan, D.; Cui, Z.; Guo, X.; Jia, J. Origin of the carbonaceous debris and its implication for mineralization within the Qianjiadian uranium deposit, southern Songliao Basin. *Ore Geol. Rev.* **2019**, *107*, 336–352. [CrossRef]
18. Rong, H.; Jiao, Y.; Liu, W.; Cao, M.; Yu, J.; Wu, L.; Li, Q. Influence mechanism of palaeoclimate of uranium-bearing strata on mineralization: A case study from the Qianjiadian sandstone-hosted uranium deposit, Songliao Basin, China. *Ore Geol. Rev.* **2021**, *138*, 104336. [CrossRef]
19. Rong, H.; Jiao, Y.; Wu, L.; Zhao, X.; Cao, M.; Liu, W. Effects of igneous intrusions on diagenesis and reservoir quality of sandstone in the Songliao Basin, China. *Mar. Pet. Geol.* **2021**, *127*, 104980. [CrossRef]
20. Qin, M.; Huang, S.; Liu, J.; Liu, Z.; Guo, Q.; Jia, L.; Jiang, W. Hydrothermal alteration and its superimposed enrichment for Qianjiadian tabular-type uranium deposit in Southwestern Songliao Basin. *Minerals* **2021**, *12*, 52. [CrossRef]
21. Jia, J.; Rong, H.; Jiao, Y.; Wu, L.; Wang, Y.; Li, H.; Cao, M. Mineralogy and geochemistry of carbonate cement in sandstone and implications for mineralization of the Qianjiadian sandstone-hosted uranium deposit, southern Songliao Basin, China. *Ore Geol. Rev.* **2020**, *123*, 103590. [CrossRef]
22. Ding, B.; Liu, H.; Xu, D.; Qiu, L.; Liu, W. Mineralogical evidence for hydrothermal uranium mineralization: Discovery and genesis of the uranyl carbonate minerals in the BLS U deposit, SW Songliao Basin, Northeast China. *Minerals* **2023**, *13*, 339. [CrossRef]
23. Chen, Z.; Li, Q.; Shao, J.; Fang, D.; Xiao, C.; Shan, Z. Feasibility study on the exploitation of rhenium associated with in-situ leaching sandstone type uranium deposit. *Nat. Resour. Inf.* **2023**, *2*, 1–9, (In Chinese with English Abstract).
24. Tessier, A.; Campbell, P.G.C.; Bisson, M. Sequential extraction procedure for the speciation of particulate trace metals. *Anal. Chem.* **1979**, *51*, 844–851. [CrossRef]
25. Liu, J.; Yang, Z.; Yan, X.; Ji, D.; Yang, Y.; Hu, L. Modes of occurrence of highly-elevated trace elements in superhigh-organic-sulfur coals. *Fuel* **2015**, *156*, 190–197. [CrossRef]
26. Wang, X.; Zeng, F.; Deng, F.; Bian, J.; Pan, Z. Rhenium in Chinese coals, a review. *Arab. J. Geosci.* **2021**, *14*, 1411. [CrossRef]
27. Shen, L.; Tesfaye, F.; Li, X.; Lindberg, D.; Taskinen, P. Review of rhenium extraction and recycling technologies from primary and secondary resources. *Miner. Eng.* **2021**, *161*, 106719. [CrossRef]
28. Fisher, Q.J.; Cliff, R.A.; Dodson, M.H. U–Pb systematics of an Upper Carboniferous black shale from South Yorkshire, UK. *Chem. Geol.* **2003**, *194*, 331–347. [CrossRef]
29. Gleyzes, C.; Tellier, S.; Astruc, M. Fractionation studies of trace elements in contaminated soils and sediments: A review of sequential extraction procedures. *TrAC Trends Anal. Chem.* **2002**, *21*, 451–467. [CrossRef]
30. Salome, K.R.; Green, S.J.; Beazley, M.J.; Webb, S.M.; Kostka, J.E.; Taillefert, M. The role of anaerobic respiration in the immobilization of uranium through biomineralization of phosphate minerals. *Geochim. Cosmochim. Acta* **2013**, *106*, 344–363. [CrossRef]
31. Millensifer, T.A.; Sinclair, D.; Jonasson, I.; Lipmann, A. Rhenium. In *Critical Metals Handbook*; Gunn, G., Ed.; John Wiley & Sons, Ltd.: Chichester, UK, 2013; pp. 340–360.

32. Min, M.; Chen, J.; Wang, J.; Wei, G.; Fayek, M. Mineral paragenesis and textures associated with sandstone-hosted roll-front uranium deposits, NW China. *Ore Geol. Rev.* **2005**, *26*, 51–69. [CrossRef]
33. Zhao, H.; Huang, F.; Zhong, S.; Li, C.; Feng, C.; Hu, Z. The Wuliping ion-adsorption deposit, Guizhou Province, South China: A new type of rhenium (re) deposit. *Ore Geol. Rev.* **2023**, *160*, 105615. [CrossRef]
34. Bonnetti, C.; Cuney, M.; Malartre, F.; Michels, R.; Liu, X.; Peng, Y. The Nuheting deposit, Erlian Basin, NE China: Synsedimentary to diagenetic uranium mineralization. *Ore Geol. Rev.* **2015**, *69*, 118–139. [CrossRef]
35. Bonnetti, C.; Cuney, M.; Michels, R.; Truche, L.; Malartre, F.; Liu, X.; Yang, J. The multiple roles of sulfate-reducing bacteria and fe-ti oxides in the genesis of the Bayinwula roll front-type uranium deposit, Erlian Basin, NE China. *Econ. Geol.* **2015**, *110*, 1059–1081. [CrossRef]
36. Rong, H.; Jiao, Y.; Liu, X.; Wu, L.; Jia, J.; Cao, M. Effects of basic intrusions on REE mobility of sandstones and their geological significance: A case study from the Qianjiadian sandstone-hosted uranium deposit in the Songliao Basin. *Appl. Geochem.* **2020**, *120*, 104665. [CrossRef]
37. Tribovillard, N.; Algeo, T.J.; Lyons, T.; Riboulleau, A. Trace Metals as Paleoredox and paleoproductivity proxies: An update. *Chem. Geol.* **2006**, *232*, 12–32. [CrossRef]
38. Hodge, V.F.; Johannesson, K.H.; Stetzenbach, K.J. Rhenium, Molybdenum, and Uranium in groundwater from the southern Great Basin, USA: Evidence for conservative behavior. *Geochim. Cosmochim. Acta* **1996**, *60*, 3197–3214. [CrossRef]